

# Collection Efficiency of a DBD Electrostatic Precipitator under Different High Voltage Waveforms

R. Gouri<sup>1,2,3</sup>, N. Zouzou<sup>2</sup>, A. Tilmatine<sup>3</sup>, E. Moreau<sup>2</sup>, and L. Dascalescu<sup>2</sup>

<sup>1</sup>Department of Electrical Engineering, University of Béchar, Algeria

<sup>2</sup>Prime Institute, University of Poitiers-ENSMA-CNRS, France

<sup>3</sup>IRCOM Laboratory, Djillali Liabes University, Algeria

**Abstract**—This experimental work is aimed at evaluating the effects of high voltage waveform (sine, square and stair) on the collection efficiency of a wire-to-square tube electrostatic precipitator using dielectric barrier discharge. The input parameters under study are the amplitude and frequency of the high voltage, as well as the tube cross-section. The collection efficiency of the electrostatic precipitator is calculated by measuring the concentration of incense particles (average diameter of 0.32  $\mu\text{m}$ ) at the outlet using an aerosol spectrometer.

**Keywords**—Dielectric barrier discharge, electrostatic precipitation, high voltage waveform

## I. INTRODUCTION

The increasingly rigorous standards on air pollution stimulate the development of appropriate technologies for collecting the impurities present in exhaust gases [1, 2]. Thus, the use of Electrostatic Precipitators (ESPs) that would guarantee high collection efficiency with minimum capital and running costs is a big challenge.

In a previous experimental work [3-7], it has been shown that the Dielectric Barrier Discharge (DBD) can be used with success for the collection of submicron particles within the range of 0.2 to 1  $\mu\text{m}$ . In the case of a wire-to-cylinder ESP, the collection efficiency reaches 99% using ac high voltage power supply operating at industrial frequency [4], which can reduce the high capital costs. Beside this advantage, the DBD avoids arc transition phenomenon which can interfere with power supplies in the case of dc corona discharges. However, the DBD-ESP consumes much more electrical power than dc-ESP to reach the same collection efficiency [5]. Consequently, further geometrical and electrical optimizations are necessary for the DBD-ESP to reach or exceed the performance of the dc-ESP.

In addition, wire-to-cylinder geometry is not suitable for the implementation in an industrial environment, especially for high flow rates. A Wire-to-Square Tube (WST) configuration, which would allow several ESPs to operate in parallel, may be a solution to the problem of industrial scaling.

In this study, the effects of the high voltage waveform on the collection efficiency of a lab-scale WST-ESP are investigated. The discharge is generated using sine, square and stair high voltage waveforms. The parameters under study are: the amplitude and frequency of the high voltage, as well as the tube section.

## II. EXPERIMENTAL SETUP

The experimental setup is illustrated in Fig. 1. Dry clean air (relative humidity < 5%) is introduced into a custom-designed smoke generator, where burning of incense sticks generates submicron particles with a mean size of about 0.32  $\mu\text{m}$ .

The particles are entrained by the airflow through the ESP. A small amount of the exhaust is connected to a diluter with a controlled additional clean air. The particle concentration in the diluted sample is measured using an aerosol spectrometer (Pallas Aerosol Technology, Model Wellas-1000, sensor range of 0.18-40  $\mu\text{m}$ , concentration up to  $10^5$  particles/cm<sup>3</sup>). The flow rate inside the measurement cell is fixed at 5 L/min. However, the flow rate ( $Q$ ) inside the ESP is adjusted between 1.6 and 20 L/min and measured using a floating ball flow meter.

The basic configuration of the WST-ESP (Fig. 2) consists of a glass square tube (300 mm length) provided with two electrodes, one of which is grounded and the other is connected to a High Voltage (HV). The HV electrode consists of a stainless steel wire (0.20 mm in diameter) aligned on the central axis of the dielectric tube. The grounded electrode is made of aluminum tape strips (80 mm width and 80  $\mu\text{m}$  thick) and is placed on the external surface of the tube.

The power supply system consists of a high voltage power amplifier (Trek, 30/20C,  $\pm 30$  kV,  $\pm 20$  mA, slew rate of 500 V/ $\mu\text{s}$ ), a function generator (TTI, TG1010, 10 MHz), a current probe (shunt resistor of 100  $\Omega$ ), a high voltage probe (internal probe of the amplifier), and a digital oscilloscope (Lecroy 424, 200 MHz, 2 GS/s). The performance of the ESP is studied at different values of HV amplitude and frequency.

The electric power consumption ( $P_{\text{elec}}$ ) is calculated from the measurement of the current ( $i$ ) and the voltage ( $v$ ) over one cycle:

$$P_{\text{elec}} = \frac{1}{T} \int_i^{i+T} v(t) \cdot i(t) \cdot dt \quad (1)$$

where  $T$  is the waveform period.

---

Corresponding author: Nouredine Zouzou  
e-mail address: noureddine.zouzou@univ-poitiers.fr

Presented at the 12th International Conference of Electrostatic Precipitation, ICESP, in May 2011 (Nuremberg, Germany)

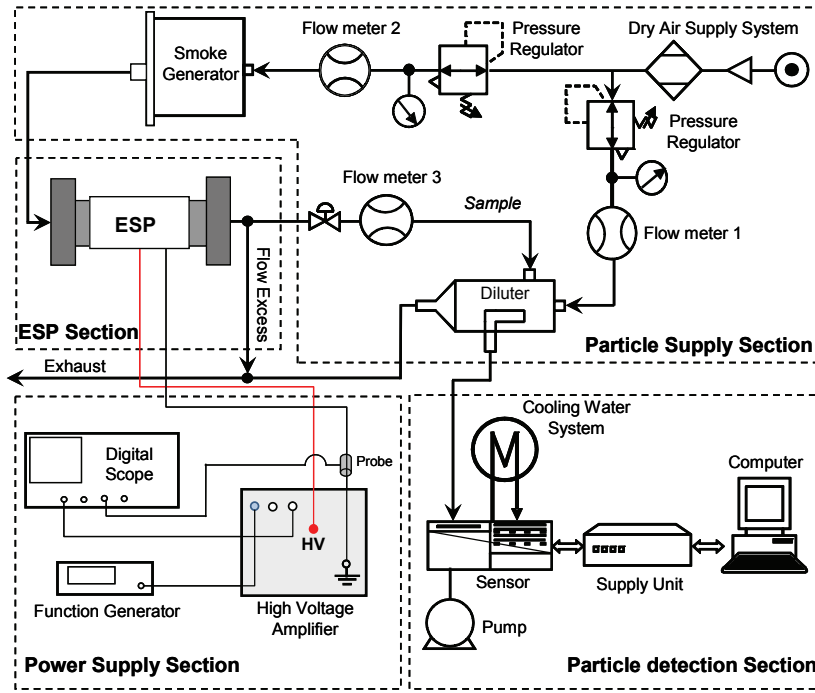


Fig. 1. Schematic illustration of the experimental setup.

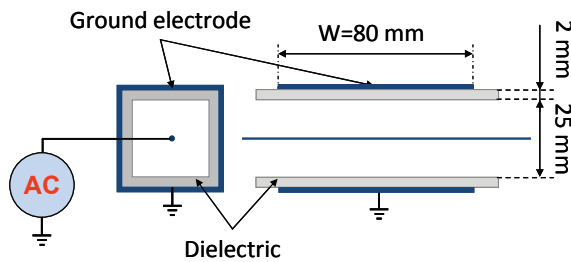


Fig. 2. Cross-view of the WST-ESP.

In practice, the time-averaged value calculated with only one cycle would not allow reaching a convergent value because it could varies from one to another cycle. In order to improve the reproducibility of the average power calculation, 10 cycles are taking into account using an acquisition memory of 250 kpts/Ch.

All the experiments are carried out at atmospheric pressure and room temperature with controlled air flow rate.

### III. RESULTS

#### A. Characterization of the WST-ESP

##### A.1. Current Waveform

The curves in Fig. 3 are typical for the time evolution of the discharge current and the applied voltage. The discharge current of the ESP includes only a few current pulses during the positive half-cycle, while there are numerous current pulses during the negative one. In the positive voltage half-cycle, the plasma is characterized by a glow-like regime. However, the Trichel pulses

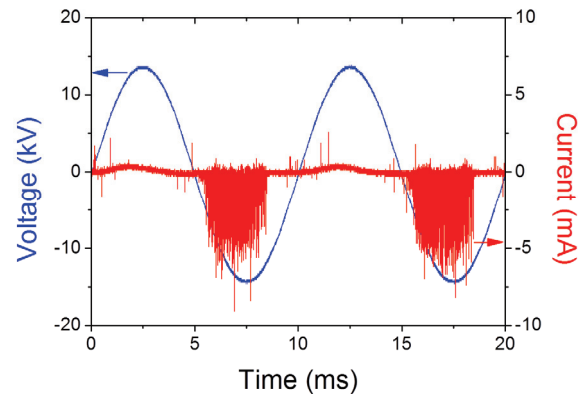


Fig. 3. Time evolution of the voltage and discharge current. Conditions:  $V_{max} = 14$  kV,  $f = 100$  Hz,  $Q = 10$  L/min.

dominate the negative voltage half cycle. Similar behavior of the DBD has been observed in point-to-plane and wire-to-cylinder configurations [8, 9].

##### A.2. Collection Efficiency

The total-number collection efficiency ( $\eta$ ) is defined as follows [10]:

$$\eta = 1 - (N_{ON}/N_{OFF}) \tag{2}$$

where  $N_{ON}$  and  $N_{OFF}$  are the numbers of particles for all size classes per  $cm^3$  with and without discharge, respectively.

To highlight the variations of the collection efficiency, especially when it is between 90% and 100%, the characterization of the precipitator is done in terms of penetration ( $P$ ):

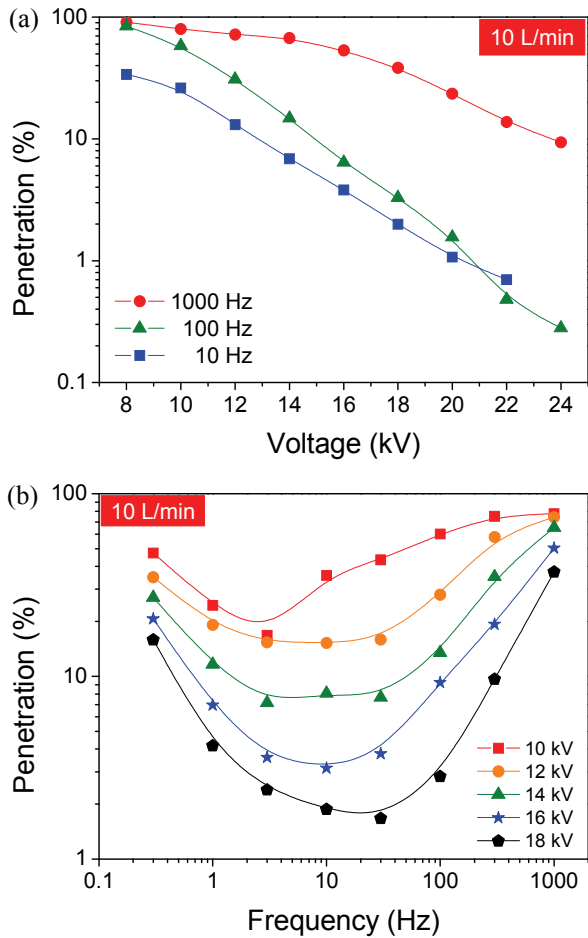


Fig. 4. Voltage (a) and frequency (b) effects on the particle penetration of the WST-ESP.

$$P = 1 - \eta \quad (3)$$

Fig. 4 (a) illustrates the evolution of particle penetration as a function of the applied voltage in log-linear scale at three frequencies (10, 100 and 1000 Hz). The collection efficiency is better at higher amplitudes of applied voltage; it can even exceed 99% (penetration less than 1%), but it is influenced by the value of the frequency, too.

*B. Effect of the Waveform on the ESP Performance*

*B.1. Current Waveform*

Fig. 5 displays the time evolution of the applied voltage and the discharge current for square and stair input waveforms. The high voltage amplitude is fixed at 14 kV. Thus, the rise and fall times (10 to 90% and 90 to 10%) are about 40  $\mu$ s for square waveform and 20  $\mu$ s for stair one. During the positive half cycles, one can clearly identify the positive glow corona although the discharge activity is depending on the input waveform. During the negative half-cycles, the Trichel pulses occur.

With both square and stair input waveforms, high current peaks occur at each positive or negative going cycles with fast rise and fall times, respectively. The

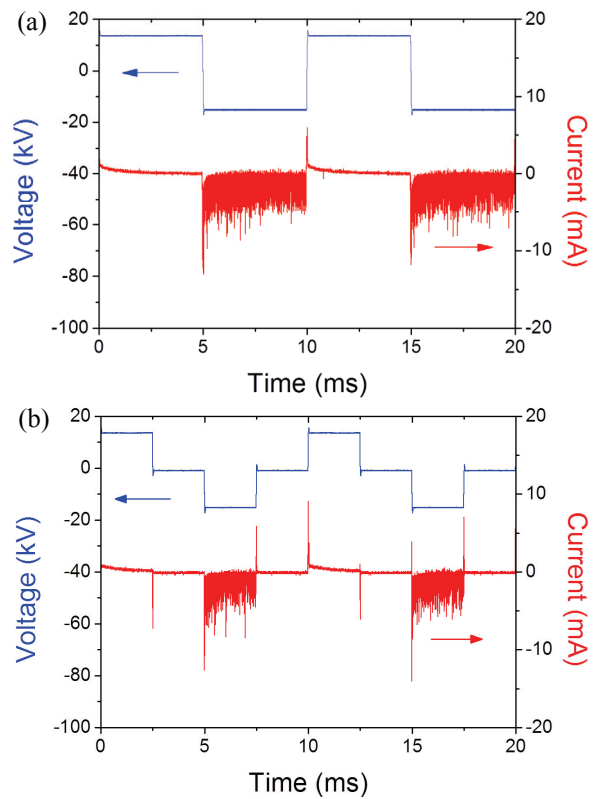


Fig. 5. Time evolution of the applied voltage and discharge current for different input waveforms: (a) Square and (b) Stair. Conditions:  $V_{max} = 14$  kV,  $f = 100$  Hz,  $Q = 10$  L/min.

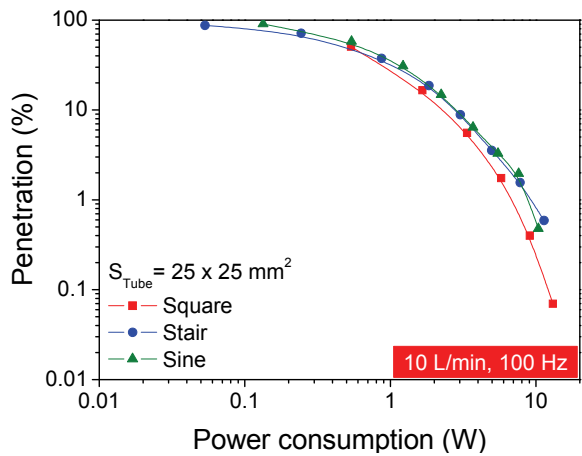


Fig. 6. Effect of high voltage waveform on the particle penetration.

positive current peaks are clearly smaller than the negative ones. They are due to the combined effect of capacitive and discharge currents. Furthermore, the duration of discharge activity varies according to the high voltage waveforms and the considered half cycle.

*B.2. Collection Efficiency*

The penetration as a function of the electric power consumption for sine, square and stair waveforms is plotted in Fig. 6. The frequency is fixed at 100 Hz.

Whatever the high voltage waveform, the ESP performance increases with the electric power consumption. Furthermore, the penetration may be lower

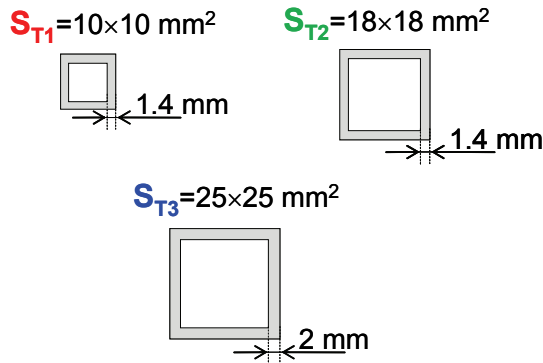


Fig. 7. Cross section view of the tested ESPs.

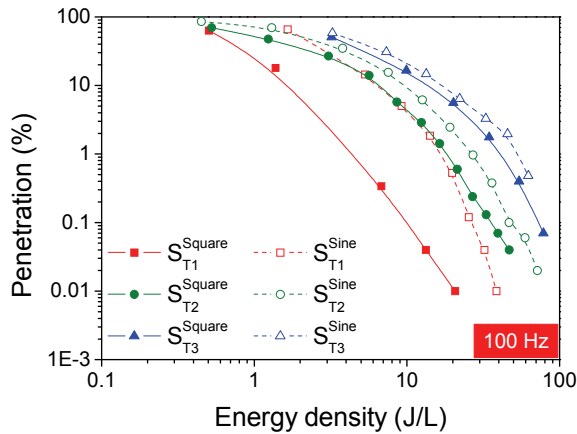


Fig. 8. Effect of the section of tube on the performance of the ESP.

than 1% for the tested waveforms if the necessary power is provided. At a given electric power, the square wave offers the best ESP performance. This is probably related to the period of discharge activity which is longer in the case of square wave. In addition, the electric field remains strong during both half cycles.

During positive or negative half-cycles, particle charging and drift processes in DBD-ESPs are close to what happen in positive or negative dc coronas, respectively. In these cases, the particles are mainly charged with the same polarity as the active wire, and then they drift toward the grounded electrodes due the electric forces and the ionic wind.

### B.3. Effect of Tube Section on the Collection Efficiency

Additional experiments were performed using three glass tubes with different internal sections ( $S_{T1} = 10 \times 10 \text{ mm}^2$ ,  $S_{T2} = 18 \times 18 \text{ mm}^2$  and  $S_{T3} = 25 \times 25 \text{ mm}^2$ ). The cross section views of these configurations are shown in Fig. 7. In order to have the same residence time of particle inside the three ESPs (about 0.3 s), the experiments were carried out at different flow rates 1.6 L/min for the first, 5.2 L/min for the second and 10 L/min for the last one.

As shown previously, the particle penetration varies with the power consumption (Fig. 6). Considering the fact that the volume of the gas treated by the three ESPs during the same time interval is different, the particle penetration is represented as a function of energy density

( $E_d$ ) as shown in Fig. 8. The energy density is defined as the power consumption divided by the flow rate:

$$E_d = P_{\text{elec}}/Q \quad (4)$$

At same energy density, the ESP performance seems to increase when using smaller sections. In addition, the difference between the performance of the ESP using sine and square waveforms is more pronounced for smaller tubes.

The results of this section are of great interest. On one hand, they demonstrate that the WST-ESP can be optimized by adjusting the applied waveform, which plays an important role on the duration of the discharge activity. On the other hand, it confirms the interest of clustering several WST-ESPs in parallel with smaller sizes.

## V. CONCLUSION

In this paper, the effect of the input waveform on the performance of a lab-scale barrier discharge ESP has been investigated in the case of wire-to-square tube configuration.

The main results are the following:

(1) For a given DBD-ESP geometry the optimum frequency of the applied high-voltage should be experimentally found. The ESP performance is poor at both low frequency, because of the intermittent nature of the discharge, and at high frequency, due to particle oscillation.

(2) The use of square high voltage waveform leads to better performances than the sine one. The fast rise time generate significant space charges, on one hand, and the electric forces remains strong during the half cycles, on the other hand.

(3) The ESP performs better with smaller tubes, especially in the case of square wave energization. Therefore, the optimum construction of DBD-ESP can be made by clustering several small-size square tubes.

## REFERENCES

- [1] J. S. Chang, "Recent development of plasma pollution control technology: A critical review," *Science and Technology of Advanced Materials*, vol. 2, pp. 571-576, 2001.
- [2] A. Mizuno, "Industrial application of atmospheric non-thermal plasma in environmental remediation," *Plasma Physics and Controlled Fusion*, vol. 49, pp. A1-A15, 2007.
- [3] B. Dramane, N. Zouzou, E. Moreau, and G. Touchard, "Characterization of a Dielectric Barrier Discharge in axisymmetric and planar configurations-Electrical-properties," *International Journal of Plasma Environmental Science & Technology*, vol. 2, pp. 89-94, 2008.
- [4] B. Dramane, N. Zouzou, E. Moreau, and G. Touchard, "Electrostatic precipitation of submicron particles using a DBD in axisymmetric and planar configuration," *IEEE Transactions on Dielectrics and Electrical Insulation*, vol. 16, pp. 343-351, 2009.
- [5] B. Dramane, N. Zouzou, E. Moreau, and G. Touchard, "Electrostatic precipitation in wire-to-cylinder configuration:

- Effect of the high-voltage power supply waveform," *Journal of Electrostatics*, vol. 67, pp. 117-122, 2009.
- [6] N. Zouzou, B. Dramane, E. Moreau, and G. Touchard, "EHD Flow and Collection Efficiency of a DBD-ESP in Wire-to-Plane and Plane-to-Plane Configurations," *IEEE Transactions on Industry Applications*, vol. 47, pp. 336-343, 2011.
- [7] R. Gouri, N. Zouzou, A. Tilmatine, E. Moreau, and L. Dascalescu, "Collection of submicron particles using DBD electrostatic precipitator in wire-to-square tube configuration," *Journal of Physics: Conference Series*, vol. 301, N°012012 (4 pp.), 2011.
- [8] M. Petit, A. Goldman, and M. Goldman, "Glow currents in a point-to-plane dielectric barrier discharge in the context of chemical reactivity control," *Journal of Physics D: Applied Physics*, vol. 35, pp. 2969-2977, 2002.
- [9] M. Abdel-Salam, A. Hashem, A. Yehia, A. Mizuno, A. Turkey, and A. Gabr, "Characteristics of corona and silent discharges as influenced by geometry of the discharge reactor," *Journal of Physics D: Applied Physics*, vol. 36, pp. 252-260, 2003.
- [10] A. Zukeran, P. C. Looy, A. Chakrabarti, A. A. Berezin, S. Jayaram, J. D. Cross, T. Ito, and J. S. Chang, "Collection efficiency of ultrafine particles by an Electrostatic Precipitator under dc and pulse operating modes," *IEEE Transactions on Industry Applications*, vol. 35, pp. 1184-1191, 1999.